Biochimie 198 (2022) 48–59

Contents lists available at ScienceDirect

Biochimie

journal homepage: www.elsevier.com/locate/biochi

Identification of an acetyl esterase in the supernatant of the environmental strain *Bacillus* sp. HR21-6

Leyre Sánchez-Barrionuevo [a, b], Jesús Mateos [c, 1], Patricia Fernández-Puente [c], Paloma Begines [d], José G. Fernández-Bolaños [d], Gabriel Gutiérrez [a], David Cánovas [a, **], Encarnación Mellado [b, *]

[a] Department of Genetics, Faculty of Biology, University of Seville, Seville, Spain
[b] Department of Microbiology and Parasitology, Faculty of Pharmacy, University of Seville, Seville, Spain
[c] Grupo de Proteómica-PBR2-ProteoRed/ISCIII. Instituto de Investigación Biomédica de A Coruña (INIBIC), Complexo Hospitalario Universitario de A Coruña (CHUAC-SERGAS). A Coruña, Spain
[d] Department of Organic Chemistry, Faculty of Chemistry, University of Seville, Seville, Spain

ARTICLE INFO

Article history:
Received 29 June 2021
Received in revised form
22 February 2022
Accepted 14 March 2022
Available online 17 March 2022

Keywords:
Esterase
Bacillus
GDSL family
Hydroxytyrosol
3,4-Dihydroxyphenylglycol
Transesterification

ABSTRACT

Bacillus sp. HR21-6 is capable of the chemo- and regioselective synthesis of lipophilic partially acetylated phenolic compounds derived from olive polyphenols, which are powerful antioxidants important in the formulation of functional foods. In this work, an acetyl esterase was identified in the secretome of this strain by non-targeted proteomics, and classified in the GDSL family (superfamily SGNH). The recombinant protein was expressed and purified from *Escherichia coli* in the soluble form, and biochemically characterized. Site-directed mutagenesis was performed to understand the role of different amino acids that are conserved among GDSL superfamily of esterases. Mutation of Ser-10, Gly-45 or His-185 abolished the enzyme activity, while mutation of Asn-77 or Thr-184 altered the substrate specificity of the enzyme. This new enzyme is able to perform chemoselective conversions of olive phenolic compounds with great interest in the food industry, such as hydroxytyrosol, 3,4-dihydroxyphenylglycol, and oleuropein.

1. Introduction

Lipases constitute a class of hydrolytic enzymes that catalyze both the hydrolysis and the transesterification of carboxylic esters. Discovering novel lipases has a great interest for food industries, as it has been demonstrated that they are efficient catalysts in different synthetic reactions performed in the presence of organic solvents [1–5].

Within the family of lipases, esterases catalyze the hydrolysis of carboxylic esters with short-length chains. Most esterases contain a serine, which has been identified as the nucleophilic residue that attacks the substrate to form an acylated intermediate. The catalytic serine residue is usually located within the classical conserved motif GXSXG. However, in members of the GDSL lipase family a different active motif located at the *N*-terminus has been identified as responsible of the catalytic activity [6]. In this latter case a serine residue was also identified as the active residue [7]. Within the GDSL lipase family, most of the esterases of the SGNH superfamily contain the conserved amino acid residues SGNH belonging to the active site and distributed in five invariant blocks. The nucleophilic serine residue is located in block I, whereas the amino acids glycine, asparagine and histidine are located in blocks II, III and V, respectively. In most cases, the serine, the aspartic acid and the histidine residues constitute the catalytic triad, and the serine (block I), the glycine (block II) and the asparagine (block III) residues compose an oxyanion hole [8].

The esterases classified among the SGNH superfamily are characterized by their multifunctional substrate specificity and regiospecificity, constituting excellent candidates as catalysts for food processing [9]. SGNH hydrolytic enzymes are found in different bacteria such as *Streptomyces rimosus* [10], *Pseudomonas aeruginosa* [11] and *E. coli* [12], and species belonging to the genus *Bacillus*

* Corresponding author.
** Corresponding author.
E-mail addresses: davidc@us.es (D. Cánovas), emellado@us.es (E. Mellado).
[1] Present address. Marine Research Institute-Spanish National Research Council (CSIC), Vigo, Spain.

https://doi.org/10.1016/j.biochi.2022.03.004

[13–16]. Although these esterases have not been studied in enough depth, their broad regio- and enantioselectivity foster a great interest of these enzymes.

The environmental lipolytic strain *Bacillus* sp. HR21-6 was previously isolated in our laboratory from food-processing industrial wastes rich in fat content. Our previous results showed that this strain is capable of chemo- and regioselective synthesis of lipophilic partially acetylated phenolic compounds derived from olive polyphenols [17]. Polyphenols are important for human health, as they have shown antioxidant, anti-inflammatory, anticancer and antidiabetic properties. Different epidemiological and clinical studies have established the health benefits of the Mediterranean diet, and that olives and olive oil are fundamental components of this diet [18–25].

In this work we identified a unique esterase (AE6L) in the soluble fraction of the secretome of the *Bacillus* sp. HR21-6. The enzyme was expressed in *E. coli* and we demonstrated experimentally that the recombinant esterase is able to perform transesterification reactions of polyphenolic compounds. Moreover, we investigated the influence of key residues identified in the SGNH family in the catalytic activity of this new enzyme.

2. Materials and methods

2.1. Bacterial strains and growth conditions

Bacillus sp. strain HR21-6 was previously isolated from food industry wastes in our laboratory using a novel screening method [17]. This strain was grown in PYB medium during 48 h at 30 °C under constant shaking to improve the enzymatic production. PYB medium contains; peptone (Intron Biotechnology) 1% (w/v), yeast extract (Intron Biotechnology) 0.5% (w/v), 5.7 mM K_2HPO_4, 4 mM $MgSO_4$. pH was adjusted to 7.5.

E. coli DH5 α (Invitrogen) and *E. coli* BL21(DE3) (Novagen) were used for genetic manipulations and protein overexpression, respectively. These strains were grown in Luria Bertani (LB) broth medium [26] at 30 °C or 37 °C under aeration conditions. The antibiotics kanamycin and streptomycin were added at 50 μg/mL and 25 μg/mL, respectively, when required.

2.2. Whole-genome sequencing of Bacillus sp. strain HR21-6

The sequencing and assembly were performed by the Genomic Functional Unit from the University of Seville (CITIUS) using a Genome Sequencer FLX System 454 (Roche) and the SOAP de novo program, version 1.05. An automatic annotation was made using the RAST server, which performs rapid annotations using subsystem technology [27].

2.3. Sequence analysis

Bioinformatics analyses of the DNA and proteins were performed using BLAST and NCBI website [28], Signal P 4.0 program [29], ProtCompB - Version 9 (http://www.softberry.com), TMHMM Server v.2.0 [30], PSIpred [31], I-TASSER [32] and PyMOL. Multiple alignments were made with Clustal Omega [33].

A search using the Batch web CD-search Tool [34,35] was conducted in order to select the homologous AE6L proteins to be included in the phylogenetic analysis. Only validated and reported sequences from different representative of the GDSL family were used. Multiple alignments were made with Clustal Omega [33]. Maximum-likelihood trees were generated using the IQ-Tree server [36]. Branch support analysis was evaluated by 1000 ultrafast bootstrap replicates and by the SH-aLRT test. ModelFinder, implemented at the IQ-Tree server was used to find the free rate heterogeneity substitution model that best fit the alignments [37]. Online tool iTOL was used to edit the constructed phylogenetic trees [38].

2.4. Identification of AE6L by secretome analysis of supernatant of Bacillus sp HR21-6

Bacillus sp. HR21-6 was grown in PYB medium at 30 °C for 24, 48 and 72 h. After a partial purification step described previously [17], the secretome analysis was performed in two fractions of the supernatant: Free Soluble Extracellular Proteins (FSEP) and Outer Membrane Vesicles (OMV), as previously described [39]. Proteins were precipitated with 10% trichloroacetic acid at 4 °C overnight. Finally, the proteins were collected by spinning at 11,500 rpm for 30 min, washed twice with cold acetone, and freeze-dried [40].

2.5. NanoLC chromatography and mass spectrometry using a 5500 QTRAP peptide selection and design of multiple reaction monitoring (MRM)

For LC-MS/MS analysis 50 μg of each protein sample freeze-dried was resuspended in 0.1 M triethylammonium bicarbonate (TEAB) buffer by vortexing and sonication. Integrity of the samples was checked by SDS-PAGE and silver staining. Standard in-solution trypsin digestion was performed with over-night trypsin incubation at 37 °C [41]. Briefly, samples were incubated with 5 μL of 200 mM TCEP ((tris(2-carboxyethyl)phosphine hydrochloride) in 0.2 ml TEAB for 1 h at 55 °C. Then 5 μL of 375 mM iodoacetamide were added to each sample and incubation was done at room temperature in the dark for 30 min. Finally 10 μL of trypsin diluted in 0.1 M TEAB was added to each sample in a 1:50 (trypsin:total protein) ratio. Samples were vortexed again and incubated overnight (not more than 16 h) at 37 °C with gentle shaking at 400 rpm. Peptide mixtures was de-salted using home-made stage-tips, aliquoted, vacuum-dried and stored at −80 °C.

Both, an Enhanced Mass and Enhanced Resolution (EM-ER) methods with a linear gradient of 120 min were performed injecting 2 μg of desalted peptide extract in the LC-MS/MS, using a nanoLC system (Tempo, Eksigent, Dublin, (CA)), USA coupled to a 5500 QTRAP platform (SCIEX). After pre-column desalting using C18 nanocolumns (C18, 5 μm, 300 A, 100 μm 2 cm, Acclaim PepMap, Thermo Scientific, USA) at a flow of 3 μL/min during 10 min, tryptic digests (2 μg) were separated (75 μm id, 15 cm, 3 μm particle size) (Acclaim PepMap 100, Thermo Scientific, USA) at a flow rate of 300 nL/min. The gradient for the EM ER method start with 5% buffer B (0.1% formic acid in 95% acetonitrile) for 3 min, with 40% of buffer B from min 3 to min 120, with 95% buffer for 1 min, hold for 10 min, and finally, equilibrated for 15 min with 5% of buffer B. Proteotypic peptides with the highest spectral counts, only fully tryptic peptides, with no missed cleavages, unique to a particular protein, with a length between 8 and 30 amino acids, devoid of methionine and tryptophan residues and missed/mis-cleavages, were chosen for MRM assay development.

The top transitions were selected using the Skyline Proteomics Environment (Mac Coss lab). In the absence of high-m/z the most abundant fragment b ions were selected. The gradient for the MRM method consisted in 5% buffer B (0.1% formic acid in 95% acetonitrile) for 3 min, followed by 35% of buffer B from min 3 to min 120, 95% buffer B for 1 min, hold for 10 min, and finally, equilibrated for 15 min with 5% buffer B. The QTRAP system was interfaced with nanospray sources equipped with uncoated fused silica emitter tips (20 μm inner diameter, 10 μm tip, New Objective, Woburn, MA) and operated in the positive ion mode. MS source parameters were: ion spray voltage (IS); 2600 V, interface heater temperature (IHT); 150 °C, ion source gas 2 (GS2); 0, curtain gas (CUR); 20, ion source

gas 1 (GS1); 25 psi, and collision gas (CAD); high. The collision energy (CE) and declustering potential (DP) was set by Skyline software and the MS compound parameters were set to 10 for the entrance potential (EP) and to 15 for the collision cell exit potential (CXP). Q1 and Q3 were set to unit/unit resolution (0.7 Da) and the pause between mass ranges was set to 3 ms.

2.6. Proteomic data analysis

Raw MS/MS data obtained from the EM-ER method were processed using the Protein Pilot 4.0 software platform (ABSciex). Peptides obtained were identified by comparison with the whole genome sequence of *Bacillus* sp. HR21-6. Search parameters were as follows: Cys-alkylation: iodoacetamide; digestion: trypsin; ID focus: biological modifications; Database: nr; Species filtering: none; Search effort: Thorough ID and Detection Protein Threshold Unused ProtScore (Conf)> 1.3 (95.0%). The scoring model was defined by the Paragon, and the False Discovery Rate was estimated by carrying out the search in parallel against a reverse nr database using PSPEP (Proteomics System Performance Evaluation Pipeline) on mode.

For the MRM study, the mass spectrometer was instructed to switch from MRM to enhanced product ion (EPI) scanning mode when an individual MRM signal exceeded 1,000 counts. Each precursor was fragmented a maximum of twice before being excluded for 10 s and the mass were scanned from 250 to 1,000 Da. MRM analysis was conducted up to 57 transitions per run (dwell time, 35 ms; cycle time or 2.5 s). Each MS/MS spectrum acquired in the 5500 QTRAP spectrometer using IDA (independent data acquisition) was searched in the in-house protein database with a low confidence threshold due to the lack of very accurate fragments to select the best peptides. Those fragments provide the best identification of the target protein using the Protein Pilot software as mentioned before. For each of the two target peptides selected, at least three transitions were monitored for each one of them and charge +2 and + 3 were monitored to confirm the co-elution of the two fragments of the same peptide. Two biological replicates of each sample were analyzed by MRM.

2.7. RNA isolation, RT-PCR, and real-time PCR

The expression levels of the *ae6l* gene were quantified by RT-qPCR. Total RNA was extracted from *Bacillus* sp. HR21-6 cells with TRIzol™ according to the instructions of the manufacturer, treated with DNase and quantified using a Nano Drop spectrophotometer (Thermo Scientific). After treatment, samples were adjusted to 12.5 ng/μl and they were used for RT-qPCR using the One-step SYBR PrimeScript RT-PCR kit (Takara Bio Inc.) according to the instructions of the manufacturer. RT-PCR was carried out using the primers indicated in Table S3 using the LightCycler 480. The fluorescent signal obtained was normalized to the corresponding fluorescent signal obtained with *gyrA* gene to correct for sampling errors using the $2^{-\Delta\Delta Ct}$ method. Similar results were found normalizing the fluorescent signal to the housekeeping gene *rpoB*.

2.8. DNA manipulation and construction of pMAB36-AE6L

Standard molecular biology techniques were employed [26]. The DNA sequence expressing the AE6L protein was synthesized *in vitro*, and it was inserted in the 6 × His-tagged pMAB36 expression vector at the *Bse*RI and *Kpn*I restriction sites. The recombinant plasmid pMAB36-AE6L-6xHis (pMAB-AE6L) was transformed to BL21(DE3) electrocompetent cells and plated onto TB-kanamycin-streptomycin agar plates. The correct sequence was confirmed by DNA sequencing.

2.9. Heterologous expression of AE6L and the different variants

Recombinant BL21(DE3) 4S2 cells including pMAB-AE6L were grown at 37 °C in TB medium added with kanamycin (50 mg/ml) and streptomycin (25 g/ml). To determine the optimum conditions for the induction of the gene, the cultures were supplemented with salicylate or isopropyl β-D-thiogalactopyranoside (IPTG) at different concentrations (0.2 and 1 mM). After induction, the *E. coli* cells were grown at 20 °C and 30 °C for 4 h to determine the optimum temperature of induction. The cells were collected by centrifugation and resuspended in TE buffer pH 7.3 (10 mM Tris-HCl, 1 mM EDTA) buffer. Finally, the recombinant cells were disrupted by ultrasonication (7 s, 150 W) on ice using a Scientz-IID sonicator (Ningbo Scientz Biotechnology, Ningbo, China). The insoluble fraction of the lysate was removed by centrifugation. The total cellular protein and soluble/insoluble protein fractions were checked by SDS-PAGE and western blot with an anti-6xHis antibody.

2.10. Purification of AE6L and the different variants

The purification of AE6L was performed from the soluble fraction obtained from biomass of 950 ml of a culture of BL21(DE3) 4S2/pMAB-AE6L, induced with 1 mM salicylate at 30 °C. Protein extracts were obtained as described above except that the buffer employed was PBS (20 mM phosphate pH 8, 150 mM NacCl). The soluble fraction was applied to Ni-agarose resin (ABT) packed in a Proteus 5 ml FliQ column (Generon, GEN-FliQ), and the purification proceeded employing a pH gradient between pH 8 and pH 4, obtained with sodium acetate buffer. Protein purity was monitored in 12% polyacrylamide SDS-PAGE gels and Comassie staining [42]. Detection of the His tagged AE6L was performed by western blot analysis using Anti-6x-His antibody (His, H8 monoclonal, Termo Fisher) and the ECL Prime Reagent detection system (GE Healthcare). Purified protein was dialyzed against TE buffer pH 7.3. The protein concentration was determined by Bradford method [43] using bovine serum albumin as standard.

2.11. Site-directed mutagenesis of the AE6L gene

Site-directed mutagenesis was performed using a Fast mutagenesis system kit (*Q5 Site-Directed Mutagenesis* Kit, New England BioLabs) using the primers indicated in Table S4. All mutation sites were confirmed by DNA sequencing. For expression, plasmids were transformed into *E. coli* BL21(DE3) cells.

2.12. Enzyme activity assays

Substrate specificity of AE6L was assayed using a set of p-nitrophenyl esters with number of carbons ranging from 2C to 18C: *p*-nitrophenyl acetate (2C), *p*-nitrophenyl butyrate (4C), *p*-nitrophenyl octanoate (8C), *p*-nitrophenyl decanoate (10C), *p*-nitrophenyl dodecanoate (12C), *p*-nitrophenyl myristate (14C), *p*-nitrophenyl palmitate (16C) and *p*-nitrophenyl estereate (18C). The activity measurement was performed in a 96-well flat bottom plate (Greiner bioOne) with a final volume of 150 μl containing 1 μg of enzyme in TE buffer pH 7.3. The plate was incubated at 37 °C for 30 min on a Fluostar OMEGA spectrophotometer (BMG Labtech) and the absorbance at 405 nm was measured every 5 min against a blank without enzyme. Enzyme activities were calculated using the molar absorption coefficient of *p*-NP (ε 5,150 M^{-1} cm^{-1}). One unit of enzyme activity was defined as the amount of enzyme required to release 1 μmole of p-nitrophenol per minute. Relative activity was calculated by dividing the enzyme activity of an enzyme variant or condition by the wild-type enzyme activity or control condition. To

determine the optimal temperature of reaction, the reactions were carried out with p-nitrophenyl acetate (2C) as substrate at 25 to 49 °C (maximum incubation temperature of the plate reader).

For study the effect of different organic solvents on the stability of the soluble enzyme, AE6L was exposed to different compounds which are normally used in industrial processes: dimethyl sulfoxide (DMSO), *N*,N-dimethylformamide, methanol, acetonitrile, ethanol, dietyl ether, acetone, 2-propanol (30% v/v 100 mM TE buffer, pH 7.3), and hexane (5% in 100 mM TE buffer, pH 7.3). The assay was carried out in the standard conditions described above. As a negative control, the soluble enzyme was used in the absence of solvents.

2.13. Determination of kinetic parameters

To determine the kinetic parameters of enzyme AE6L, the enzymatic assay was carried out using increasing concentrations (0.25, 0.5, 0.75, 1.0, 2.0 and 3 mM) of *p*-NP acetate in order to saturate the lipolytic activity of the enzyme. Subsequently, the activity was measured using the standard conditions described above. The kinetic parameters were deduced applying the kinetics of Michaelis [44], linearizing by means of the Hanes-Woolf Plot equation [45].

2.14. AE6L mediated O-deacylation of phenolic compounds

The deacylation reactions were carried out with peracetylated hydroxytyrosol 1, peracetylated 3,4-dihydroxyphenyl glycol 3 and peracetylated oleuropein 5 as previously reported [17] with some small modifications. Briefly, reactions were performed by adding the purified AE6L to a solution of compounds 1, 3 or 5 in CD_3OD (0.6 mL) using 2,000:1 substrate:enzyme at 60 °C for 5, 8 and 24 h and following the reactions by ^1H NMR. For compound 3 the reaction was also assayed at 1,000:1 and 400:1 substrate:enzyme ratio. Finally, the solvent was evaporated, and the residue was purified by column chromatography to obtain compounds 2, 4 or 6. The structure of the formed compounds was confirmed by ^1H and ^{13}C NMR. No reaction was observed in the absence of the enzyme.

2.15. Sequences accession numbers

The nucleotide sequence of the genome is deposited under accession number PRJEB34473.

3. Results

3.1. Bacillus sp. HR21-6 genome sequencing and bioinformatic analysis

In order to identify the putative lipases and esterases that could be responsible for the acylation/deacylation of phenolic compounds, firstly the complete genome of *Bacillus* sp. HR21-6 was sequenced. The genome sequence was assembled into 63 contigs, and a total genome size of 3,727,231 bps. The G+C content of the genome was estimated to be 41.26%, which falls within the typical range of genomes of *Bacillus* species. The genome was annotated using the RAST server, and it contained a total of 4,068 predicted genes. Among the annotated ORFs 6 lipases and 30 esterases were predicted.

3.2. Analysis of exoproteome of Bacillus sp. HR21-6. Identification of AE6L

Since the number of lipases and esterases was too high for an individual analysis, we decided to analyze the secretome of *Bacillus sp.* HR21-6 by non-targeted proteomics with the aim of identifying all the putative proteins that could mediate the deacetylation of the phenolic compounds previously described [17]. The strain was grown in PYB medium at 30 °C for 24, 48 and 72 h. The supernatants were fractionated to isolate the outer membrane vesicles (OMVs) and the free soluble extracellular proteins (FSEP). These fractions were analyzed separately by SDS-PAGE and silver staining (Fig. 1a). As expected, a different protein pattern was observed between OMVs and FSEP. Consequently, the analysis of the exoproteome was performed using both the OMVs and FSEP samples of *Bacillus sp.* HR21-6. A similar protein pattern was detected in the three incubation times tested for each fraction. We selected 48 h of growth, because previous work pointed to a maximum of enzymatic activity at this time point [17].

In order to identify the secreted proteins, in-solution trypsin-digested samples (2 μg) were analyzed by Liquid Chromatography coupled to Mass Spectrometry (LC-MS) in a 5500 QTRAP platform (SCIEX) using an EMER (Enhanced Mass-Enhanced Resolution) shotgun proteomics approach. A total of 48 and 28 different proteins were identified in the FSEP and OMV fractions, respectively (Table S1). Out of those 76 proteins only one esterase isoform (three peptides) (peg.2639_rhamnogalacturonan acetylesterase) was detected in FSEP, which was absent in the OMV samples. No lipases were identified in any of the fractions of the supernatant during the analysis. The gene, annotated as a rhamnogalacturonan acetylesterase, was identified in the contig 16 of the genome of *Bacillus sp.* HR21-6. The sequence analysis of the gene showed an open reading frame of 672 bp in length that encodes a protein of 223 amino acids. The protein was named AE6L. The predicted molecular mass and pI were 26 kDa and 5.06, respectively. The gene encoded a protein without a predicted signal sequence using the SignalP 4.0 server. However, the ProtCompB (Version 9) software predicted that AE6L is secreted with score of 8.4 (http://www.softberry.com), in agreement with its detection in the exoproteome of *Bacillus* sp. HR21-6.

To confirm this result, a Multiple Reaction Monitoring (MRM) targeted proteomics analysis of this acetyl-esterase was performed. Two proteotypic peptides (charge +2 and + 3 of GATPLLLTPVGR and YTAQGVSVDNR) were monitored for co-elution of at least three transitions each. In FSEP samples all the transitions co-elute at the same retention times with good intensity signal (Figs. 1b and S1). In the case of the OMV samples, there was no elution of the transitions for the peptides at the same retention time than in the FSEP samples. Besides, no fragmentation spectrum data are available for this protein. Taken altogether, an acetyl-esterase isoform was detected and identified in the FSEP samples using both shotgun and targeted proteomics methodologies.

To determine the expression pattern of the AE6L gene that encodes the acetyl-esterase of interest, *Bacillus sp*. HR21-6 was grown on PYB medium at different times of incubation, and the expression was assessed by RT-qPCR (Fig. 1c). The expression of the gene peaked at 24 h of incubation, compared to the expression levels observed at the other incubation times. This expression peak preceded the time at which the protein was identified in the culture supernatant.

3.3. Sequence analysis of AE6L

The exploration of the conserved domains in this protein was performed using the CDD database at NCBI. This analysis predicted that AE6L contains a conserved domain common in all hydrolases of the superfamily SGNH belonging to the lipase family II/GDSL [6], and an acetyl esterase domain, typical of the carbohydrate esterase family CE-12. AE6L showed the highest sequence similarity to esterases of *Bacillus* species for which no information on their

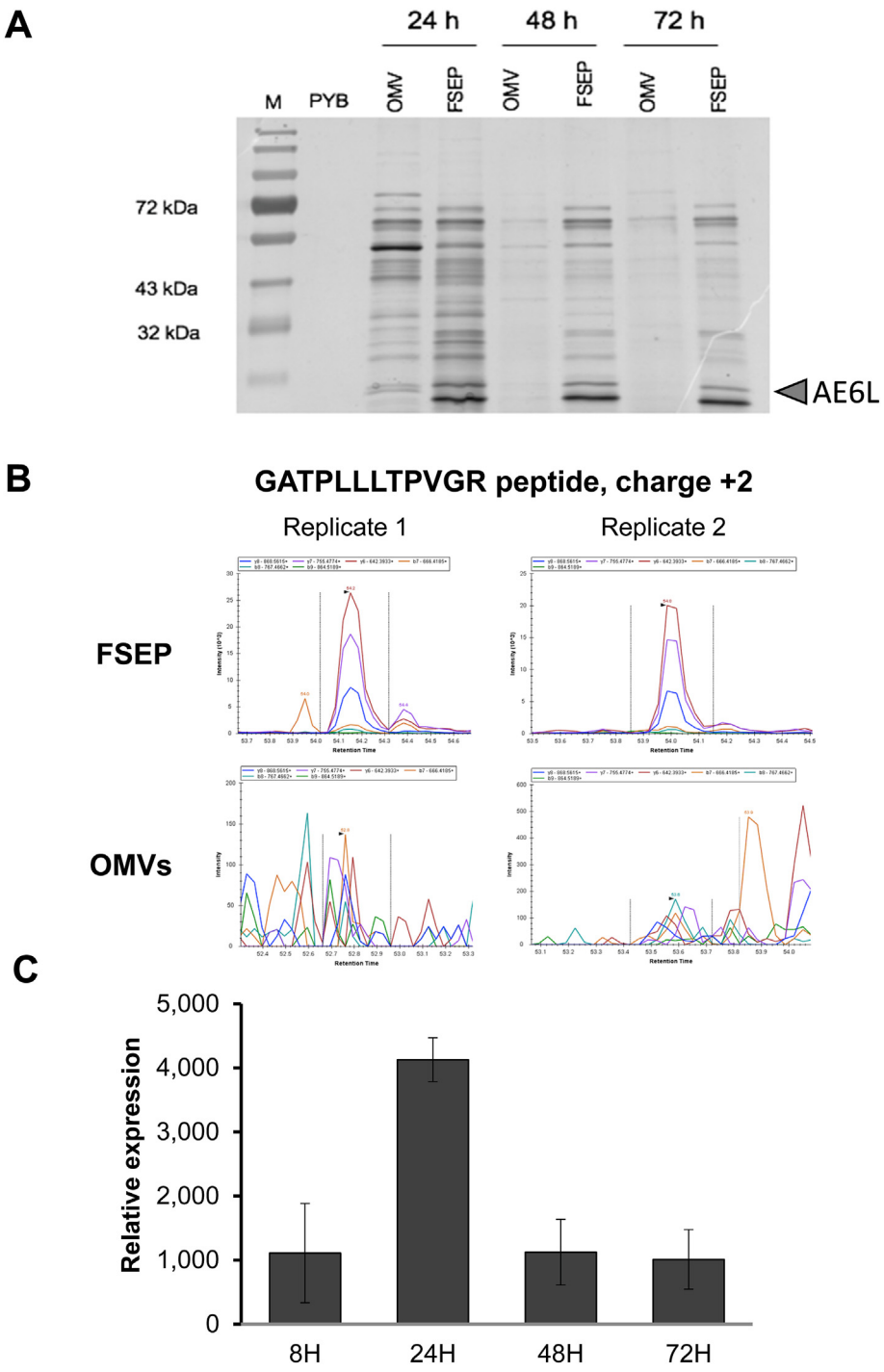

Fig. 1. Detection and quantification of AE6L expression. A) SDS-PAGE analysis of proteins present in the FSEP and OMV fractions of the supernatant of *Bacillus* sp. HR21-6 collected at different growth times and stained with silver nitrate, M. Molecular mass marker. PYB. Culture medium used as control. B) MRM analysis of the +2-charged GATPLLLTPVGR peptide of the acetyl esterase detected in the FSEP fraction of the supernatant of *Bacillus* sp. HR21-6. C) Expression of *ae6l* gene in *Bacillus sp*. HR21-6 quantified by RT-qPCR. The strain was grown on PYB medium at different times. The expression levels were normalized using the expression of the *gyrA* gene.

biochemical characteristics and functions have been reported (Table S2).

To explore the evolutionary relationships between AE6L and other GDSL hydrolases belonging to different genera a phylogenetic tree was constructed (Fig. 2). AE6L clustered together with other esterases from *Bacillus* species, with the only exception of the esterase of *Erwinia (Dickeya) chrysantemi*, a gamma-proteobacteria.

3.4. Expression and purification of AE6L

The AE6L gene (672 bp) was synthesized and cloned into the expression vector pMAB36 obtaining a fusion protein with a *N*-terminal $(His)_6$ tag. The codon usage was adapted for expression in *E. coli* to facilitate protein expression. The recombinant plasmid (pMAB36-AE6L) was transformed into *E. coli* BL21(DE3) as host cell

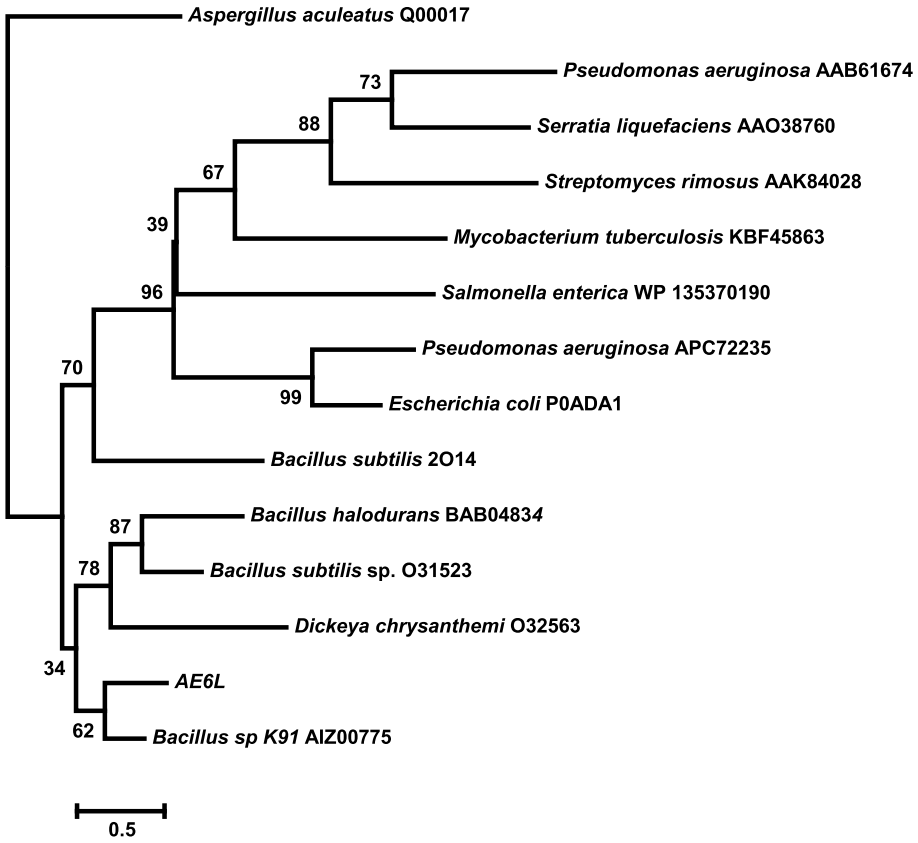

Fig. 2. Phylogenetic analysis of AE6L and related enzymes of the GDSL lipase family. The tree shows the phylogenetic relationships of 13 representative lipolytic enzymes of the superfamily GDSL and AE6L from *Bacillus* sp. HR21-6. Multiple alignments were made employing Clustal Omega. The maximum-likelihood tree was generated using the IQ-Tree server. Branch support analysis was evaluated by 1,000 ultrafast bootstrap replicates. ModelFinder was used to find the free rate heterogeneity substitution model that best fit the alignment and on line iTOl was used for tree editing.

to facilitate high levels of protein expression. SDS-PAGE gel electrophoresis showed an overexpression band corresponding to a protein of approx. 26 kDa, which is compatible with the size of AE6L. The conditions for expression were optimized. The highest expression was found with 1 mM salicylate at 30 °C for 4 h (Supplementary Fig. 2a) and the protein was expressed in the soluble form (Supplementary Fig. 2b).

The recombinant 6xHis-tagged AE6L was purified by Ni-IMAC chromatography from the soluble fraction of the *E. coli* recombinant strain. The purified AE6L migrated in SDS-PAGE as a single band consistent with its calculated molecular weight (approx. 26 kDa), which was confirmed by Western blotting. The purification process rendered a solution of 0.179 mg/ml of purified AE6L with a specific activity of 39.64 U/mg (using *p*-NP acetate as a substrate). Based on the relative quantification by Western blot the yield of the purification was 60%.

3.5. Biochemical characterization of AE6L esterase

The substrate specificity of purified AE6L was assayed under the standard conditions established testing the hydrolytic activity against different *p*-nitrophenol esters with acyl chain lengths ranging from 2C to 18C. The purified enzyme displayed a preference for short-chain fatty acids, yielding the highest activity with *p*-NP acetate (39.64 U/mg). The hydrolytic activity of the enzyme dropped drastically with *p*-nitrophenol esters of chain lengths longer than 2C (Fig. 3a).

Analysis of the kinetics of AE6L using *p*-NP acetate (2C) as a substrate at pH 7.3 and 37 °C revealed a typical Michaelis-Menten kinetics with K_m value of 1.7 mM, a V_{max} of 13.600 μmol min^{-1}. The k_{cat} was 777.12 min^{-1} and a catalytic efficiency (k_{cat}/k_m) 457.12 min^{-1} $mmol^{-1}$.

The influence of temperature on the *p*-NP acetate hydrolyzing activity was tested over a range from 25 to 49 °C in TE buffer at pH 7.3. The enzyme was most active at 30–37 °C. An abrupt decrease of activity was observed at temperatures above 37 °C, although at 49 °C AE6L still maintained approx. 40% of the maximum activity (Fig. 3b).

As most of the industrial processes are produced in the presence of organic solvents, we analyzed the stability of the enzyme AE6L in presence of different hydrophobic and hydrophilic solvents. We used a battery of organic solvents at a concentration of 30%, except the hexane that was used at a concentration of 5%. Although a decrease in the activity was detected in all the organic compounds tested, AE6L showed the best results in presence of dimethyl sulfoxide (DMSO). The stability in methanol and other alcohols is convenient for transesterification reactions, as shown below (Fig. 3c).

3.6. Design of mutations and production of AE6L mutants

A sequence alignment was performed with the AE6L enzyme and the more related proteins. This comparison allowed us to identify the presence of the four conserved blocks including the putative catalytic triad (Ser-10, Asp-181 and His-184), which were described to play specific roles in the catalytic function of the enzyme [6]. Moreover, the GDSL(X) motif (Gly-8, Asp-9, Ser-10, Thr-11) was identified in block I close to the *N*-terminus of the protein

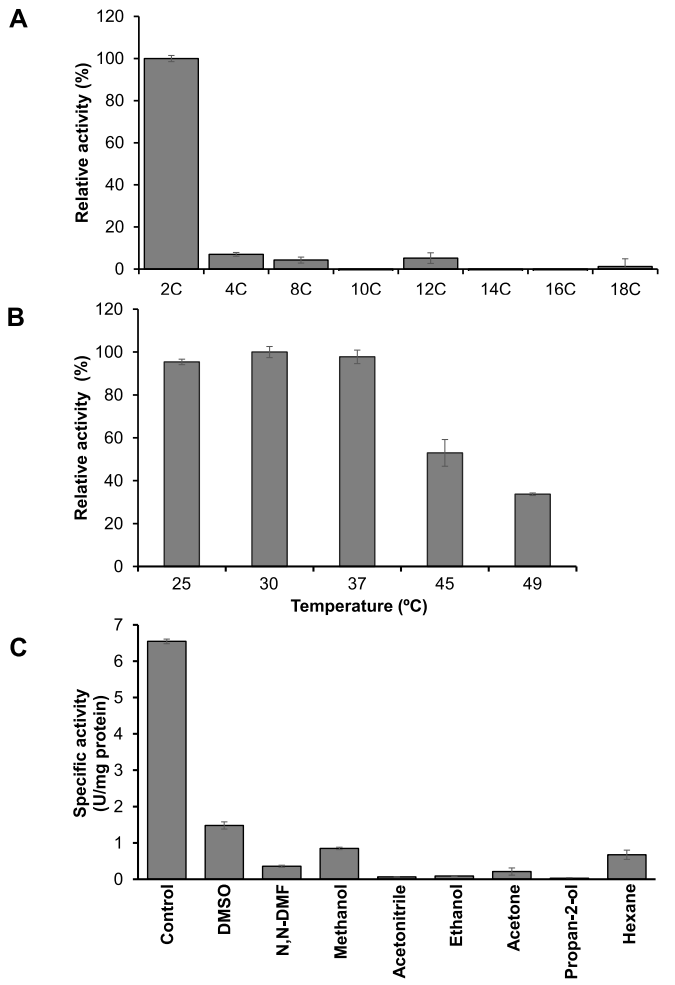

Fig. 3. Biochemical characterization of AE6L. A) Substrate specificity of AE6L towards *p*-NP esters with different acyl chain lengths (C2–C18). The activity was measured using the standard assay (pH 7.3 at 37 °C). B) Effect of temperature on the activity of AE6L. The activity was assayed using *p*-NP-acetate as substrate at pH 7.3. C) Effect of different organic solvents on AE6L activity using *p*-NP acetate as substrate and pH 7.3 at 37 °C. *N*,N-DMF: N′,N-dimetilformamide. Data shown are the average of three independent experiments and the standard deviation of the mean.

(Supplementary Fig. 3). A structural model of AE6L was created using I-TASSER and the acetylesterase AaRGAE from *Aspergillus aculeatus* (PDB code 1deo) as structural template, which displays a 27% identity to AE6L (Table S2). The homology modeling analysis revealed some features that are similar in both proteins. The putative residues Gly-45 and Asn-77 could form an oxyanion hole with Ser-10, suggesting again that AE6L could be classified as a member of the SGNH superfamily of hydrolases (Fig. 4a).

Based on this analysis of the structure we selected the four conserved residues of AE6L identified as putative amino acids involved in the hydrolytic reactions: Ser-10, Gly-45, Asp-181 and His-184, conforming the key consensus sequences in this family of esterases [6]. These four amino acids were substituted by alanine by site-directed mutagenesis. Additionally, the amino acids Asn-77 and Thr-183 described as motifs involved in the specificity of substrate [8,46] were also substituted by alanine to examine the influence of substrate side-chain size on the biochemical properties of the enzyme. Two additional residues were selected: Glu-26, which was substituted by glutamine, the most frequent residue in that position in the esterases of this family; and Ser-96, one amino acid that is present in this position exclusively in AE6L, which was substituted by alanine.

The residues selected for mutagenesis were located in the 3D model of AE6L (Fig. 4a). Ser-10, Asp-181 and His-184 are located close to each other in the structure and lined up in a side of the catalytic cleft, Gly-45 and Asn-77 are located in loops close to the active site, and Ser-96 and Glu-26 were located on the protein surface far from the active site.

AE6L wild-type and mutants were expressed in *E. coli* BL21(DE3) (Fig. 4b), and the presence of the AE6L wild-type and mutant versions was confirmed by western blot analysis (Fig. 4c).

3.7. Characterization of the AE6L variants

The catalytic activity of the eight mutants was tested and compared with wild-type AE6L using *p*-NP acetate as substrate. AE6L variants S10A, G45A and H184A located in the invariants blocks I, II and V of the SGNH family of lipases, respectively, completely lost their activity to hydrolyze *p*-NP acetate, suggesting a critical role for these residues in the catalytic activity. However, the AE6L variants N77A and D181A located in blocks III and V, respectively, and described as donors of protons during the catalytic reaction, did not result in the complete loss of activity using *p*-NP acetate as substrate. According to this result, these residues did not seem to be essential in the catalytic activity on *p*-NP acetate (Fig. 5a).

To analyze how the mutations affect the specificity of AE6L for the substrates, we determined the specific activities of AE6L and some selected variants (N77A, D181A, S96A, E26Q and T183A) employing *p*-NP esters of fatty acids of different chain lengths. With substrates of chain lengths greater than 12C (*p*-NP dodecanoate), a general loss of activity was observed in all the mutants tested (data not shown). Compared to the AE6L (WT), the variants N77A and T183A were more active towards esters of longer fatty acids chains, being the effect on *p*-NP octanoate (8C) more significant in the N77A variant (Fig. 5b). It is noteworthy that although Asn-77 has been described as a residue implicated in the catalytic activity donating protons during the reaction, the mutant N77A showed activities in *p*-NP octanoate (8C) comparable to those of AE6L in *p*-NP acetate. This result suggests that, in AE6L the Asn-77 residue is likely to be involved in substrate specificity rather than in the catalytic reaction *per se*.

The variant E26Q showed a recovery of the activity when using *p*-NP with longer acyl chain lengths, being more significant in *p*-NP octanoate (8C). The variant S96A showed similar levels of activity from 2C to 8C decreasing in the case of longer C chains (Fig. 5b).

To analyze the influence of the temperature in the mutants, we determined the optimal temperature of each mutant and compared to the wild type (AE6L). Similar to the wild type (AE6L), all the mutants presented the maximum activity at 25-30 °C (Fig. 5c). However, while the wild type showed the maximum activity at 37 °C, a decrease in the activity was observed in all the mutants tested at 37 °C (and higher temperatures). The variant S96A showed lower decrease of the activity at 45 °C and 49 °C than the wild-type version (Fig. 5c).

3.8. Regioselective deacylation of polyphenols using AE6L

To test the performance of the novel AE6L esterase as a catalyst in chemoselective biotransformations in the food industry, we used different polyphenolic compounds present in olives with demonstrated excellent antioxidant properties, such as hydroxytyrosol **1**, 3,4-dihydroxyphenylglycol (DHPG) **3**, and oleuropein **5**. A previous study demonstrated that chemoselective deacetylation of the peracetylated derivatives of hydroxytyrosol and DHPG was far more efficient than chemoselective acetylation of the compounds *per se*

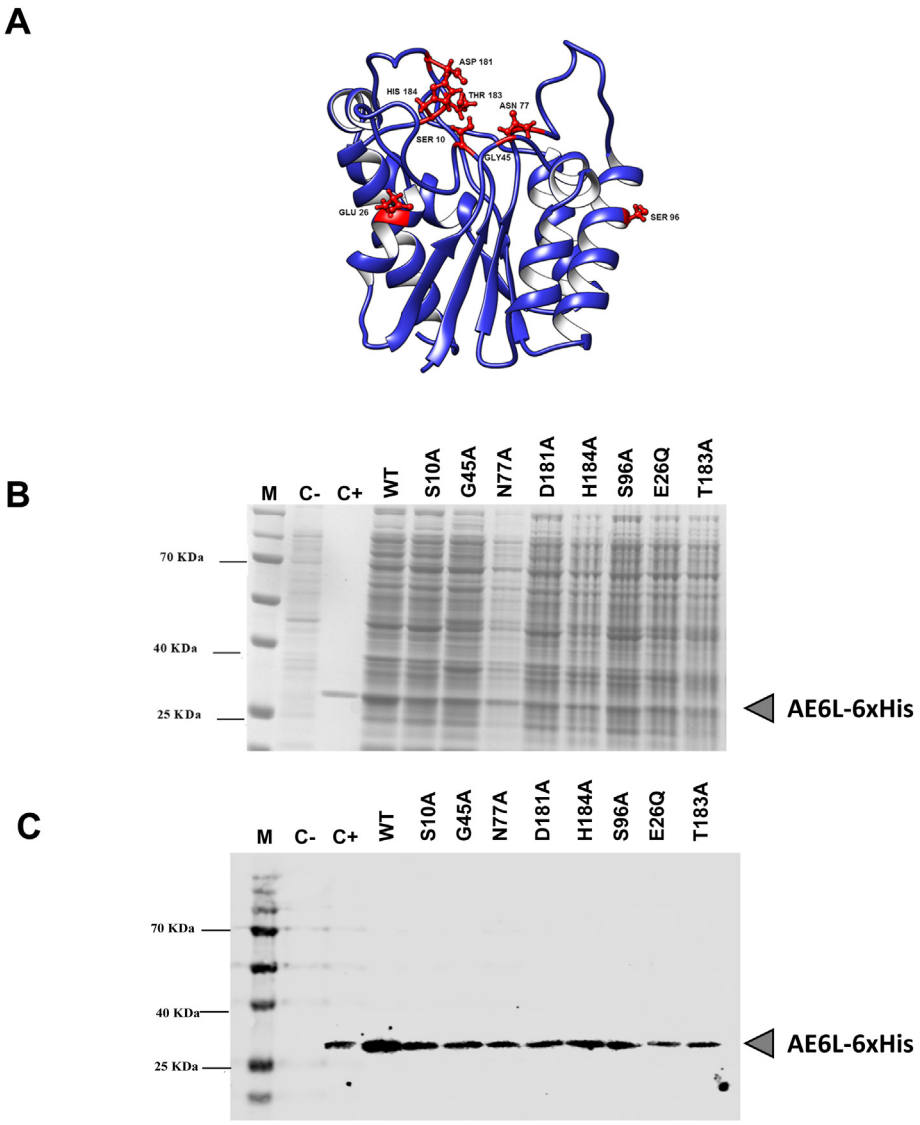

Fig. 4. Design and production of AE6L mutant versions. A) Location of the amino acids selected for mutagenesis in the 3D model of AE6L performed in i-Tasser. B) The wild-type (WT) and the mutant versions were expressed in *E. coli* and proteins in the total cell extract were visualized by coomassie brilliant blue-stained gel. C) Western blot detection of the wild-type and mutant proteins with an anti-6xHis antibody. M, molecular weight marker. *C-*, *E. coli* BL21 (DE3) pMAB-AE6L without inducing. C +, pure AE6L. WT, pMAB-AE6L. S10A, pMAB-AE6LS10A. G45A, pMAB-AE6LG45A. N77A, pMAB-AE6LN77A. D182A, pMAB-AE6LD182A. H185A, pMAB-AE6LH185A. S96A, pMAB-AE6LS96A. E26Q, pMAB-AE6LE26Q. T184A, pMAB-AE6LT184A. Polyacrylamide gels (12% w/v) were stained with Coomassie brilliant blue. AE6L protein and variants, indicated by the arrow, was identified according to the estimated mass from SDS–PAGE compared with the estimated mass from the amino acid sequence.

[17]. Therefore, all these compounds were peracetylated as described in material and methods, and used as substrates in deacetylation reactions employing the purified enzyme AE6L. All the reactions (using the three peracetylated substrates) were conducted at 60 °C as we observed lower conversion values in reactions performed a lower temperature (data not shown). The conversion yields were measured by NMR at different times (5 h, 8 h and 24 h) to analyze the reaction time course.

The deacetylation of peracetylated hydroxytyrosol **1** was conducted in a transacetylation reaction with methanol (as an aliphatic alcohol) in a mixture containing 2000:1 (W/W) substrate:enzyme (Table 1). The reaction was completely chemoselective towards the aromatic positions, giving a monoacetylated derivative **2** in the aliphatic position (Fig. 6). The amounts of product increased along with the reaction time, obtaining the maximum yield (49%) after 24 h (Table 1).

When peracetylated DHPG **3** was employed as substrate, we observed again that the aromatic hydroxyl groups were chemoselectively deacetylated by a transacetylation reaction employing methanol as a solvent, leading to compound **4**, in a reaction mixture including 2,000:1 substrate:enzyme (Table 1). The acetoxy group at the primary position remained unchanged, whereas the acetoxy at benzylic position was substituted by a methoxy group (Fig. 6). This is a remarkable reaction, which was previously described with the whole supernatants of *Bacillus* sp. HR21-6 [17]. The data obtained here with the purified AE6L revealed that the esterase AE6L is one of the enzymes in the supernatant of *Bacillus* sp. HR21-6 required for the exchange of the acetoxy by a methoxy group, and the consequent conversion of an ester into an ether group.

Oleuropein is an interesting molecule, since it contains both a phenolic moiety and a sugar moiety (Fig. 6). The deacetylation of peracetylated oleuropein 5 also showed a chemoselective reaction, producing the selective deacetylation of phenolic acetyl moieties, whereas the acetyl groups on the sugar moiety remained intact.

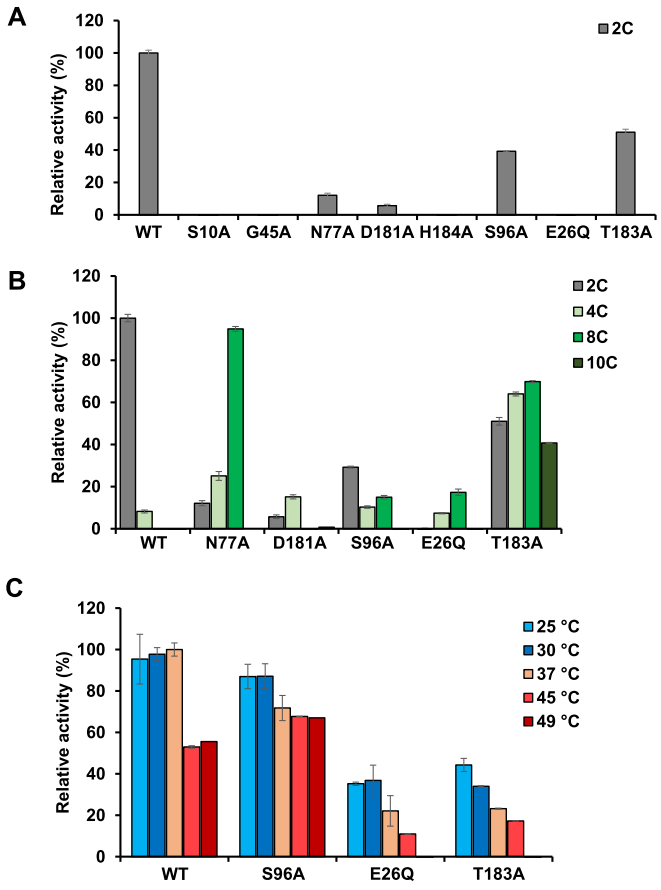

Fig. 5. Characterization of the AE6L variants. A) Relative activity (%) of mutants with respect to AE6L (WT) at 37 °C and using *p*-NP acetate (2C). **(B–C)** Relative activity (%) of active mutants with respect to AE6L (WT) at 37 °C employing derivatives of *p*-NP with different chain lengths (B) and different temperatures (C). The activity was normalized by subtracting the activity of the negative control, *E. coli* BL21(DE3). The substrates used were *p*-NP acetate (C2), *p*-NP butyrate (C4), *p*-NP octanoate (C8), and *p*-NP decanoate (C10). Data shown are the average of three independent experiments and the standard deviation of the mean.

Table 1
O-Deacetylation of polyphenolic compounds catalyzed by AE6L at 60 °C.

	Conversion %		
Compound	5 h[a]	8 h	24 h
Peracetylated hydroxytyrosol **1**	8	21	49
Peracetylated DHPG **3**	8	12	22[b]
Peracetylated oleuropein **5**	14	20	45

Substrate/enzyme (w/w) 2000/1 in CD_3OD as solvent (0.6 mL). No reaction was observed in the absence of the enzyme.
[a] Reaction time.
[b] Using a substrate/enzyme (w/w) 400/1, the conversion was 53% after 24 h.

This reaction gave the tetraacetylated oleuropein 6 (Fig. 6) as a single product with a maximum yield (45%) after 24 h (Table 1). It was also observed that the chain length of the acyl donor significantly influenced the performance of AE6L in the transesterification reactions using DHPG, as the enzyme appeared to be very active in transesterification reactions in methanol, but not in the presence of other alcohols with longer chains (data not shown). In the case of the deacetylation of peracetylated DHPG 2, the conversions obtained using ethanol as solvent were very reduced, even increasing the amount of AE6L in the reaction and employing longer reaction times.

4. Discussion

Phenolic components in olives and olive oil have important health-promoting effects [47–52]. However, their applications as supplements in dietary formulations in non-aqueous media are limited due to their hydrophilic character. We previously described a simple and low-cost procedure using partially purified extracts of *Bacillus* sp. HR21-6 to perform chemoselective and regioselective synthesis of lipophilic acetylated derivatives of some phenolic compounds extracted from olives [17]. Due to the promising results obtained during this previous study we proceeded with the identification of a unique acetyl esterase, named AE6L, by a nontargeted proteomics approach. AE6L was found in the FESP of *Bacillus* sp. HR21-6. The catalytic efficiency of AE6L toward *p*-NP acetate (2C) was at least 14 and 23-fold higher than toward *p*-NP butyrate (4C) and *p*-NP octanoate (8C), respectively. No significant hydrolase activity was detected for the substrates with acyl-chain-length higher than 8C. These results indicate that AE6L is an esterase rather than a lipase.

AE6L is a new GDSL esterase that clusters with members of the SGNH family including other esterases from *Bacillus* and *Dickeya* (Fig. 2). AE6L is more active towards short-chain *p*-NP esters as found in other GDSL family bacterial lipases previously characterized [13,15,16]. In addition, we identified the characteristic sequence features shared with the esterases assigned to the GDSL family, such as the presence of the catalytic triad (Ser-10, Asp-181 and His-184). The enzyme does not exhibit the conventional pentapeptide Gly-X-Ser-X-Gly typical of the conventional lipases, although a serine residue is included in the GDSL(X) consensus motif (Gly-8, Asp-9, Ser-10, Thr-11) serving as the catalytic nucleophile and the hydrogen proton donor to the oxyanion hole. Replacement of the Ser-10 by Ala completely abolished the esterase activity of AE6L towards *p*-NP acetate (Fig. 5A) and other esters (data not shown). The key role of serine in homologous proteins has been previously described as responsible for the nucleophilic attack, which is in agreement with our results here. The Ala replacement of the other two residues in catalytic triad (Asp-181 and His-184) gave different results. His-184 acts by deprotonating serine [6,53], and its mutation also produced a completely inactive AE6L. Mutation of Asp-181 did not abolish the activity of the enzyme completely using *p*-NP acetate as the substrate. mutation of either Asn-77 or Asp-181 increased its activity towards substrates of longer chain. It was proposed that Asp-181 is close to the entrance of the tunnel, and can affect the accessibility of the substrates to the pocket [46], which would explain the change in the substrate specificity found in $AE6L^{D181A}$, in addition to the drastic reduction of the enzymatic activity.

In the SGNH lipase superfamily the catalytic Ser-10 is located much closer to the *N*-terminus than in other lipolytic enzymes, and together with the residues Gly-45 and Asn-77 assemble an oxyanion hole [6], which therefore has three hydrogen-bond donors. The mutation of amino acid Asn-77 in the oxyanion hole did not completely abolish the activity of the enzyme when using *p*-NP acetate as substrate, presumably because the lack of one of the residues in the oxyanion hole can be replaced by the other. Two thirds of the hydrogen-bonding remained intact, which should have provided two thirds of the activity. However, only 12% of the activity was retained towards *p*-NP acetate. Interestingly, we found that mutation of Asn-77 increased its activity towards substrates of longer chain. Although this can be surprising, as Asn-77 was supposed to be involved in the donation of protons in the active center, similar results were found in the case of *E. coli* TAP (thioesterase I, EC 3.1.2.2) [46]. Asn-77 is close to a switch loop essential for the accommodation of substrates and it was proposed to be essential for the accommodation of longer acyl-chain-length substrates [46],

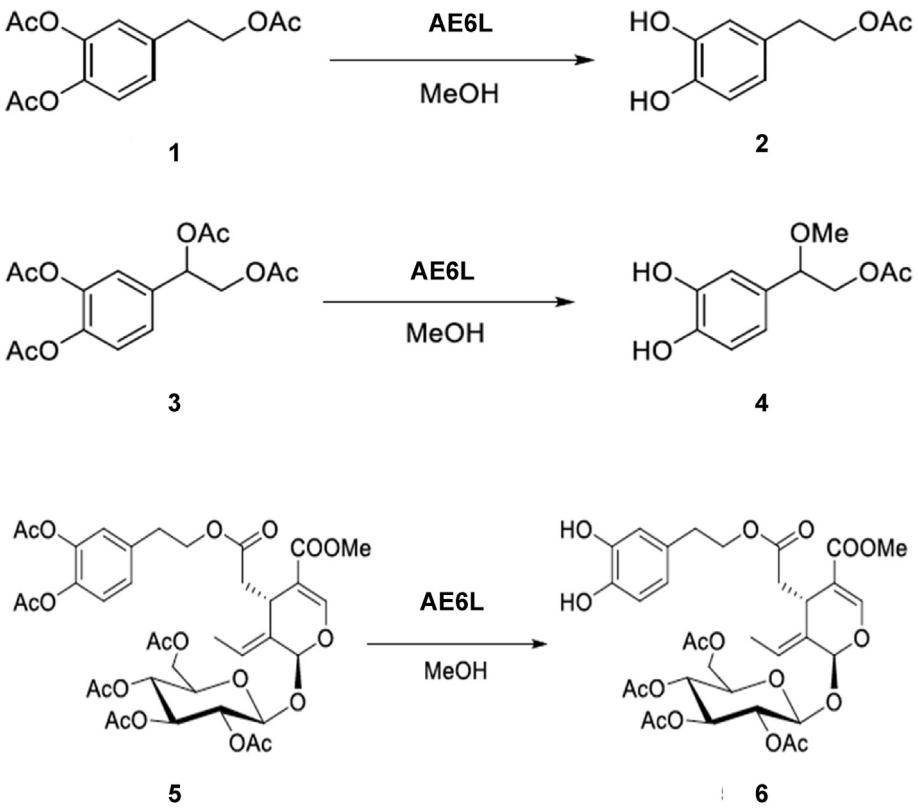

Fig. 6. Chemoselective *O*-deacetylation of peracetylated hydroxytyrosol **1**, DHPG **3** and oleuropein **5** catalyzed by AE6L.

as we have observed in AE6L^{N77A}. This proposition is compatible with the results obtained for AE6L, where the activity of AE6L^{N77A} towards *p*-NP octanoate (C8) was comparable to the activity of the wild-type variants towards *p*-NP acetate (C2). The mutation of Thr-183, which is also located in the oxyanion hole, also increased the length of the carbon chain of the substrate that the enzyme can accommodate. In this case, the T183A variant had a relative activity of 70% for C8 and 40% for C10 compared to the wild-type for C2. Changes in the specificity of substrate were also observed in the lipases SXL from *Staphylococcus xylosus* and SSL from *Staphylococcus simulans* by replacing the Asp290 residue for Ala [54,55] and by replacing the Gly311 residue in the SXL lipase for Leu, Trp, Asp or Lys [54].

Our analysis also revealed the importance of two other residues Glu-26 and Ser-96 for the activity of AE6L. The E26Q and S96A variants showed a loss of activity, being more significant in the case of Glu-26, clearly indicating the importance of this amino acid in the catalytic activity, even though it is not conserved in the alignment with different proteins of this esterase family. The case of E26Q is intriguing as this mutation is naturally present in other rhamnogalacturonan esterases (Fig. S3), and it was predicted to be neutral using the PROVEAN software [56] and stabilizing using the DynaMut2 [57]. AE6L^{E26Q} is still active towards *p*-NP butyrate (C4) and *p*-NP octanoate (C8) but not towards *p*-NP acetate (C2), which suggests that changes in this helix may affect the conformation of the oxyanion hole, accommodating other type or length of substrates.

The optimum temperature for activity of the purified AE6L was 30–37 °C, and the enzyme retained approx. a 40% of activity at 49 °C. The variants E26Q, S96A and T183A lead to a decrease in the optimal reaction temperature in comparison of AE6L, showing the maximum activity at 25-30 °C. Interestingly, the S96A mutation retained its activity in the whole range of temperatures (30-49 °C) analyzed and conferred 1.2 times more activity at the highest temperature analyzed (49 °C) compared with AE6L (Fig. 5c).

It has been described that the GDSL esterases have multifunctional activities with several industrial applications (due to the flexibility exhibited in the active site allowing a broad substrate specificities, such as complex polysaccharides, acyl-CoA esters and more complex compounds) [58,59]. In fact, several GDSL lipases have been described to be useful in asymmetric synthesis, such as the lipase from *Xanthomonas vesicatoria* [60] or the lipase from *Marinactinospora thermotolerans* [40]. A previous report showed that the supernatants of *Bacillus* sp. HR21-6 were capable of transesterification reactions of polyphenolic compounds [17].

In the present study we included hydroxytyrosol, DHPG and oleuropein as substrates for the analysis of transesterification reactions. Hydroxytyrosol is a classical and powerful antioxidant found in olive oil by-products [61] DPHG is a poorly studied polyphenol structurally related to HT but more efficient as antioxidant than hydroxytyrosol [62] and oleuropein is a secoiridoide glucoside, which have been selected as the molecule contains a hydroxytyrosol moiety, constituting the major phenolic component of the leaves and green olives. This compound has great interest due to its antioxidant, anti-apoptotic and vasodilator properties [63,64].

Our results indicate that the purified AE6L had a higher reaction yield than the supernatants of *Bacillus* sp HR21-6 employed in the previous work [17], requiring three orders of magnitude lower amounts of the enzyme compared to the supernatants. The reaction produced lipophilic partially acetylated derivatives (Fig. 6), which preserved the antioxidant characteristics, avoiding the tedious conventional methods for the synthesis of these derivatives. It is noteworthy the results obtained in the deacylation of the

oleuropeine, leading to a total chemoselectivity towards the phenolic fraction of the molecule (Fig. 6), remaining intact the glucosidic part of the molecule, and the other two esters present in oleuropein, the one connecting hydroxytyrosol with the secoiridoid moiety and the methoxycarbonyl function.

5. Conclusions

This work expands the diversity of the SGNH subfamily, an unexploited group of esterases, showing that this new enzyme is able to perform chemoselective conversions of polyphenolic compounds with great interest in the food industry. AE6L was classified in the SGNH subfamiliy. Three residues (Ser-10, Gly-45 and His-184) were identified as essential for the enzymatic activity by site-directed mutagenesis and constitute the active triad. Our results also indicate that two other amino acids (Asn-77 and Thr-183) participate in substrate specificity and the mutation of any of three amino acids Glu-26, Ser-96 or Thr-183 affects the optimal temperature of reaction**.** We have explored the chemoenzymatic synthesis as a powerful tool for accessing these valuable derivatives in a non-expensive and green fashion to produce nutritional ingredients.

Author contributions

LSB carried out the purification, biochemical characterization and bioinformatics work. JM and PFP performed the experiments concerning the proteomic data analysis and critically reviewed the manuscript. PB and JMFB performed the transesterification reactions. GG was responsible of data curation. DC and EM conceived the project, wrote the manuscript and were responsible for project administration and funding acquisition. All authors read and approved the manuscript.

Funding information

This work was supported by Junta de Andalucía (P11-CVI-7427 MO).

Declaration of competing interest

The authors declare that there are no competing interests associated with the manuscript.

Acknowledgements

We acknowledge the financial support of the Junta de Andalucía (P11-CVI-7427 MO).

Appendix A. Supplementary data

Supplementary data to this article can be found online at https://doi.org/10.1016/j.biochi.2022.03.004.

References

[1] K.E. Jaeger, T. Eggert, Lipases for biotechnology, Curr. Opin. Biotechnol. 13 (2002) 390–397.
[2] D.G. Filho, A.G. Silva, C.Z. Guidini, Lipases: sources, immobilization methods, and industrial applications, Appl. Microbiol. Biotechnol. 103 (2019) 7399–7423.
[3] P. Priyanka, Y. Tan, G.K. Kinsella, G.T. Henehan, B.J. Ryan, Solvent stable microbial lipases: current understanding and biotechnological applications, Biotechnol. Lett. 41 (2019) 203–220.
[4] L. Ramnath, B. Sithole, R. Govinden, Classification of lipolytic enzymes and their biotechnological applications in the pulping industry, Can. J. Microbiol. 63 (2017) 179–192.
[5] P. Chandra, Enespa, R. Singh, P.K. Arora, Microbial lipases and their industrial applications: a comprehensive review, Microb. Cell Factories 19 (2020) 169.
[6] C.C. Akoh, G.C. Lee, Y.C. Liaw, T.H. Huang, J.F. Shaw, GDSL family of serine esterases/lipases, Prog. Lipid Res. 43 (2004) 534–552.
[7] C. Upton, J.T. Buckley, A new family of lipolytic enzymes? Trends Biochem. Sci. 20 (1995) 178–179.
[8] A. Molgaard, S. Kauppinen, S. Larsen, Rhamnogalacturonan acetylesterase elucidates the structure and function of a new family of hydrolases, Structure 8 (2000) 373–383.
[9] I. Lescic Asler, N. Ivic, F. Kovacic, S. Schell, J. Knorr, U. Krauss, S. Wilhelm, B. Kojic-Prodic, K.E. Jaeger, Probing enzyme promiscuity of SGNH hydrolases, Chembiochem : a Europ. j. chem. biol. 11 (2010) 2158–2167.
[10] I. Lescic Asler, Z. Stefanic, A. Marsavelski, R. Vianello, B. Kojic-Prodic, Catalytic dyad in the SGNH hydrolase superfamily: in-depth insight into structural parameters tuning the catalytic process of extracellular lipase from *Streptomyces rimosus*, ACS Chem. Biol. 12 (2017) 1928–1936.
[11] F. Kovacic, J. Granzin, S. Wilhelm, B. Kojic-Prodic, R. Batra-Safferling, K.E. Jaeger, Structural and functional characterisation of TesA - a novel lysophospholipase A from *Pseudomonas aeruginosa*, PLoS One 8 (2013), e69125.
[12] Y.C. Lo, S.C. Lin, J.F. Shaw, Y.C. Liaw, Crystal structure of *Escherichia coli* thioesterase I/protease I/lysophospholipase L1: consensus sequence blocks constitute the catalytic center of SGNH-hydrolases through a conserved hydrogen bond network, J. mol. biol. 330 (2003) 539–551.
[13] J. Ding, T. Yu, L. Liang, Z. Xie, Y. Yang, J. Zhou, B. Xu, J. Li, Z. Huang, Biochemical characterization of a GDSL-motif esterase from *Bacillus* sp. K91 with a new putative catalytic mechanism, J. Microbiol. Biotechnol. 24 (2014) 1551–1558.
[14] J. Ding, H. Zhu, Y. Ye, J. Li, N. Han, Q. Wu, Z. Huang, Z. Meng, A thermostable and alkaline GDSL-motif esterase from *Bacillus* sp. K91: crystallization and X-ray crystallographic analysis, Acta crystallogr. Section F, Struct. biol. commun. 74 (2018) 117–121.
[15] I. Martinez-Martinez, J. Navarro-Fernandez, J. Daniel Lozada-Ramirez, F. Garcia-Carmona, A. Sanchez-Ferrer, YesT: a new rhamnogalacturonan acetyl esterase from *Bacillus subtilis*, Proteins 71 (2008) 379–388.
[16] J. Navarro-Fernandez, I. Martinez-Martinez, S. Montoro-Garcia, F. Garcia-Carmona, H. Takami, A. Sanchez-Ferrer, Characterization of a new rhamnogalacturonan acetyl esterase from *Bacillus halodurans* C-125 with a new putative carbohydrate binding domain, J. Bacteriol. 190 (2008) 1375–1382.
[17] L. Sanchez-Barrionuevo, A. Gonzalez-Benjumea, A. Escobar-Nino, M.T. Garcia, O. Lopez, I. Maya, J.G. Fernandez-Bolanos, D. Canovas, E. Mellado, A straightforward access to new families of lipophilic polyphenols by using lipolytic bacteria, PLoS One 11 (2016), e0166561.
[18] A. Cilla, G. De Palma, M.J. Lagarda, R. Barbera, R. Farre, G. Clemente, F. Romero, Impact of fruit beverage consumption on the antioxidant status in healthy women, Ann. Nutr. Metab. 54 (2009) 35–42.
[19] A. Coccia, L. Mosca, R. Puca, G. Mangino, A. Rossi, E. Lendaro, Extra-virgin olive oil phenols block cell cycle progression and modulate chemotherapeutic toxicity in bladder cancer cells, Oncol. Rep. 36 (2016) 3095–3104.
[20] C. Grossi, S. Rigacci, S. Ambrosini, T. Ed Dami, I. Luccarini, C. Traini, P. Failli, A. Berti, F. Casamenti, M. Stefani, The polyphenol oleuropein aglycone protects TgCRND8 mice against Ass plaque pathology, PLoS One 8 (2013), e71702.
[21] I. Luccarini, T. Ed Dami, C. Grossi, S. Rigacci, M. Stefani, F. Casamenti, Oleuropein aglycone counteracts Abeta42 toxicity in the rat brain, Neurosci. Lett. 558 (2014) 67–72.
[22] M.A. Rosillo, M.J. Alcaraz, M. Sanchez-Hidalgo, J.G. Fernandez-Bolanos, C. Alarcon-de-la-Lastra, M.L. Ferrandiz, Anti-inflammatory and joint protective effects of extra-virgin olive-oil polyphenol extract in experimental arthritis, J. Nutr. Biochem. 25 (2014) 1275–1281.
[23] C. Santangelo, C. Filesi, R. Vari, B. Scazzocchio, T. Filardi, V. Fogliano, M. D'Archivio, C. Giovannini, A. Lenzi, S. Morano, R. Masella, Consumption of extra-virgin olive oil rich in phenolic compounds improves metabolic control in patients with type 2 diabetes mellitus: a possible involvement of reduced levels of circulating visfatin, J. Endocrinol. Invest. 39 (2016) 1295–1301.
[24] D. Vauzour, G. Corona, J.P. Spencer, Caffeic acid, tyrosol and *p*-coumaric acid are potent inhibitors of 5-S-cysteinyl-dopamine induced neurotoxicity, Arch. Biochem. Biophys. 501 (2010) 106–111.
[25] M. Gorzynik-Debicka, P. Przychodzen, F. Cappello, A. Kuban-Jankowska, A. Marino Gammazza, N. Knap, M. Wozniak, M. Gorska-Ponikowska, Potential health benefits of olive oil and plant polyphenols, Int. J. Mol. Sci. 19 (2018).
[26] M.R. Green, J. Sambrook, Molecular Clonning. A Laboratory Manual, fourth ed. ed., Cold Spring Harbor Laboratory Press2012.
[27] R.K. Aziz, D. Bartels, A.A. Best, M. DeJongh, T. Disz, R.A. Edwards, K. Formsma, S. Gerdes, E.M. Glass, M. Kubal, F. Meyer, G.J. Olsen, R. Olson, A.L. Osterman, R.A. Overbeek, L.K. McNeil, D. Paarmann, T. Paczian, B. Parrello, G.D. Pusch, C. Reich, R. Stevens, O. Vassieva, V. Vonstein, A. Wilke, O. Zagnitko, The RAST Server: rapid annotations using subsystems technology, BMC Genom. 9 (2008) 75.
[28] S.F. Altschul, W. Gish, W. Miller, E.W. Myers, D.J. Lipman, Basic local alignment search tool, J. mol. biol. 215 (1990) 403–410.
[29] J.D. Bendtsen, H. Nielsen, G. von Heijne, S. Brunak, Improved prediction of signal peptides: SignalP 3.0, J. mol. biol. 340 (2004) 783–795.
[30] A. Krogh, B. Larsson, G. von Heijne, E.L. Sonnhammer, Predicting transmembrane protein topology with a hidden Markov model: application to complete genomes, J. mol. biol. 305 (2001) 567–580.
[31] L.J. McGuffin, K. Bryson, D.T. Jones, The PSIPRED protein structure prediction server, Bioinformatics 16 (2000) 404–405.

[32] A. Roy, A. Kucukural, Y. Zhang, I. TASSER, A unified platform for automated protein structure and function prediction, Nat. Protoc. 5 (2010) 725–738.
[33] F. Sievers, A. Wilm, D. Dineen, T.J. Gibson, K. Karplus, W. Li, R. Lopez, H. McWilliam, M. Remmert, J. Soding, J.D. Thompson, D.G. Higgins, Fast, scalable generation of high-quality protein multiple sequence alignments using Clustal Omega, Mol. Syst. Biol. 7 (2011) 539.
[34] A. Marchler-Bauer, Y. Bo, L. Han, J. He, C.J. Lanczycki, S. Lu, F. Chitsaz, M.K. Derbyshire, R.C. Geer, N.R. Gonzales, M. Gwadz, D.I. Hurwitz, F. Lu, G.H. Marchler, J.S. Song, N. Thanki, Z. Wang, R.A. Yamashita, D. Zhang, C. Zheng, L.Y. Geer, S.H. Bryant, CDD/SPARCLE: functional classification of proteins via subfamily domain architectures, Nucleic Acids Res. 45 (2017) D200–D203.
[35] A. Marchler-Bauer, S. Lu, J.B. Anderson, F. Chitsaz, M.K. Derbyshire, C. DeWeese-Scott, J.H. Fong, L.Y. Geer, R.C. Geer, N.R. Gonzales, M. Gwadz, D.I. Hurwitz, J.D. Jackson, Z. Ke, C.J. Lanczycki, F. Lu, G.H. Marchler, M. Mullokandov, M.V. Omelchenko, C.L. Robertson, J.S. Song, N. Thanki, R.A. Yamashita, D. Zhang, N. Zhang, C. Zheng, S.H. Bryant, CDD: a conserved domain database for the functional annotation of proteins, Nucleic Acids Res. 39 (2011) D225–D229.
[36] J. Trifinopoulos, L.T. Nguyen, A. von Haeseler, B.Q. Minh, W.-I.Q. TREE, A fast online phylogenetic tool for maximum likelihood analysis, Nucleic Acids Res. 44 (2016) W232–W235.
[37] S. Kalyaanamoorthy, B.Q. Minh, T.K.F. Wong, A. von Haeseler, L.S. Jermiin, ModelFinder: fast model selection for accurate phylogenetic estimates, Nat. Methods 14 (2017) 587–589.
[38] I. Letunic, P. Bork, Interactive tree of life (iTOL) v3: an online tool for the display and annotation of phylogenetic and other trees, Nucleic Acids Res. 44 (2016) W242–W245.
[39] C. Rumbo, E. Fernandez-Moreira, M. Merino, M. Poza, J.A. Mendez, N.C. Soares, A. Mosquera, F. Chaves, G. Bou, Horizontal transfer of the OXA-24 carbapenemase gene via outer membrane vesicles: a new mechanism of dissemination of carbapenem resistance genes in *Acinetobacter baumannii*, Antimicrob. Agents Chemother. 55 (2011) 3084–3090.
[40] D. Deng, Y. Zhang, A. Sun, J. Liang, Y. Hu, Functional characterization of a novel marine microbial GDSL lipase and its utilization in the resolution of (+/-)-1-phenylethanol, Appl. Biochem. Biotechnol. 179 (2016) 75–93.
[41] P. Fernandez-Puente, J. Mateos, F.J. Blanco, C. Ruiz-Romero, LC-MALDI-TOF/TOF for shotgun proteomics, Methods Mol. Biol. 1156 (2014) 27–38.
[42] U.K. Laemmli, Cleavage of structural proteins during the assembly of the head of bacteriophage T4, Nature 227 (1970) 680–685.
[43] M.M. Bradford, A rapid and sensitive method for the quantitation of microgram quantities of protein utilizing the principle of protein-dye binding, Anal. Biochem. 72 (1976) 248–254.
[44] L. Michaelis, M.L. Menten, K.A. Johnson, R.S. Goody, The original Michaelis constant: translation of the 1913 Michaelis-Menten paper, Biochemistry 50 (2011) 8264–8269.
[45] C.S. Hanes, Studies on plant amylases: the effect of starch concentration upon the velocity of hydrolysis by the amylase of germinated barley, Biochem. J. 26 (1932) 1406–1421.
[46] L.C. Lee, Y.L. Lee, R.J. Leu, J.F. Shaw, Functional role of catalytic triad and oxyanion hole-forming residues on enzyme activity of *Escherichia coli* thioesterase I/protease I/phospholipase L1, Biochem. J. 397 (2006) 69–76.
[47] M.I. Covas, K. Nyyssonen, H.E. Poulsen, J. Kaikkonen, H.J. Zunft, H. Kiesewetter, A. Gaddi, R. de la Torre, J. Mursu, H. Baumler, S. Nascetti, J.T. Salonen, M. Fito, J. Virtanen, J. Marrugat, The effect of polyphenols in olive oil on heart disease risk factors: a randomized trial, Ann. Intern. Med. 145 (2006) 333–341.
[48] M. Deiana, G. Corona, A. Incani, D. Loru, A. Rosa, A. Atzeri, M. Paola Melis, M. Assunta Dessi, Protective effect of simple phenols from extravirgin olive oil against lipid peroxidation in intestinal Caco-2 cells, Food Chem. Toxicol. : int. j. publi. Brit. Ind. Biol. Res. Associat. 48 (2010) 3008–3016.
[49] I. Kalaiselvan, M. Samuthirapandi, A. Govindaraju, D. Sheeja Malar, P.D. Kasi, Olive oil and its phenolic compounds (hydroxytyrosol and tyrosol) ameliorated TCDD-induced heptotoxicity in rats via inhibition of oxidative stress and apoptosis, Pharmaceut. Biol. 54 (2016) 338–346.
[50] A.M. Borzi, A. Biondi, F. Basile, S. Luca, E.S.D. Vicari, M. Vacante, Olive oil effects on colorectal cancer, Nutrients (2018) 11.
[51] A. Karkovic Markovic, J. Toric, M. Barbaric, C. Jakobusic Brala, Hydroxytyrosol, tyrosol and derivatives and their potential effects on human health, Molecules (2019) 24.
[52] P. Reboredo-Rodriguez, A. Varela-Lopez, T.Y. Forbes-Hernandez, M. Gasparrini, S. Afrin, D. Cianciosi, J. Zhang, P.P. Manna, S. Bompadre, J.L. Quiles, M. Battino, F. Giampieri, Phenolic compounds isolated from olive oil as nutraceutical tools for the prevention and management of cancer and cardiovascular diseases, Int. J. Mol. Sci. 19 (2018).
[53] Y.S. Ho, L. Swenson, U. Derewenda, L. Serre, Y. Wei, Z. Dauter, M. Hattori, T. Adachi, J. Aoki, H. Arai, K. Inoue, Z.S. Derewenda, Brain acetylhydrolase that inactivates platelet-activating factor is a G-protein-like trimer, Nature 385 (1997) 89–93.
[54] H. Mosbah, A. Sayari, S. Bezzine, Y. Gargouri, Expression, purification, and characterization of His-tagged *Staphylococcus xylosus* lipase wild-type and its mutant Asp 290 Ala, Protein Expr. Purif. 47 (2006) 516–523.
[55] A. Sayari, H. Mosbah, Y. Gargouri, Importance of the residue Asp 290 on chain length selectivity and catalytic efficiency of recombinant *Staphylococcus simulans* lipase expressed in *E. coli*, Mol. Biotechnol. 36 (2007) 14–22.
[56] Y. Choi, G.E. Sims, S. Murphy, J.R. Miller, A.P. Chan, Predicting the functional effect of amino acid substitutions and indels, PLoS One 7 (2012), e46688.
[57] C.H.M. Rodrigues, D.E.V. Pires, D.B. Ascher, DynaMut2: assessing changes in stability and flexibility upon single and multiple point missense mutations, Protein Sci 30 (2021) 60–69.
[58] R. Millar, R. Rahmanpour, E.W.J. Yuan, C. White, T.D.H. Bugg, Esterase EstK from *Pseudomonas putida* mt-2: an enantioselective acetylesterase with activity for deacetylation of xylan and poly(vinylacetate), Biotechnol. Appl. Biochem. 64 (2017) 803–809.
[59] F. Wang, H. Zhang, Z. Zhao, R. Wei, B. Yang, Y. Wang, Recombinant lipase from *Gibberella zeae* exhibits broad substrate specificity: a comparative study on emulsified and monomolecular substrate, Int. J. Mol. Sci. 18 (2017).
[60] D. Talker-Huiber, J. Jose, A. Glieder, M. Pressnig, G. Stubenrauch, H. Schwab, Esterase EstE from *Xanthomonas vesicatoria* (Xv_EstE) is an outer membrane protein capable of hydrolyzing long-chain polar esters, Appl. Microbiol. Biotechnol. 61 (2003) 479–487.
[61] R.M. de Pablos, A.M. Espinosa-Oliva, R. Hornedo-Ortega, M. Cano, S. Arguelles, Hydroxytyrosol protects from aging process via AMPK and autophagy; a review of its effects on cancer, metabolic syndrome, osteoporosis, immune-mediated and neurodegenerative diseases, Pharmacol. Res. 143 (2019) 58–72.
[62] G. Rodriguez, A. Lama, S. Jaramillo, J.M. Fuentes-Alventosa, R. Guillen, A. Jimenez-Araujo, R. Rodriguez-Arcos, J. Fernandez-Bolanos, 3,4-Dihydroxyphenylglycol (DHPG): an important phenolic compound present in natural table olives, J. Agric. Food Chem. 57 (2009) 6298–6304.
[63] C.D. Goldsmith, D.R. Bond, H. Jankowski, J. Weidenhofer, C.E. Stathopoulos, P.D. Roach, C.J. Scarlett, The olive biophenols oleuropein and hydroxytyrosol selectively reduce proliferation, Influence the cell cycle, and induce apoptosis in pancreatic cancer cells, Int. J. Mol. Sci. 19 (2018).
[64] S.H. Omar, Cardioprotective and neuroprotective roles of oleuropein in olive, Saudi Pharmaceut. J. : SPJ : the off. publi. Saudi Pharm. Soc. 18 (2010) 111–121.